Eigenmodes of metallic ring systems: A rigorous approach

Lei Zhou[1,*] and S. T. Chui[2]
[1]*Surface Physics Laboratory (State Key Laboratory) and Physics Department, Fudan University, Shanghai 200433, People's Republic of China*
[2]*Bartol Research Institute, University of Delaware, Newark, Delaware 19716, USA*
(Received 27 February 2006; revised manuscript received 3 June 2006; published 17 July 2006)

To study the eigenmodes of a metallic system in ring geometry, we develop an approach which *rigorously* considers all inductive/capacitive effects within the quasistatic approximation. Application to a single-ring split ring resonator (SRR) reveals that the odd-numbered modes exhibit both magnetic and electric responses while the even ones only exhibit electric responses, and the SRR shows a bianisotropy for the odd-numbered resonances. Symmetry restriction allows a plane wave to excite only certain resonance modes of a SRR. Simulations on realistic structures verify all theoretical predictions. Calculations for a double-ring case suggest "optic (acoustic) modes" of asymmetric bianisotropy that are much more electric (magnetic) in character.

DOI: 10.1103/PhysRevB.74.035419 PACS number(s): 78.20.Bh, 41.20.Jb, 42.60.Da, 78.67.−n

I. INTRODUCTION

There is much recent interest in the scattering of electromagnetic (EM) waves from collections of nanoelements, partially motivated by recently discovered left-handed materials (LHM's).[1] A modular approach to investigate such problems consists of studying the circuit characteristics of individual constitutive elements. When different elements are combined to form a new structure, some characteristics need not be recalculated. This approach complements other approaches in that it provides for easier understanding of the scattering properties of structures, particularly when some constitutive elements are changed.

It is not commonly appreciated that for any element the circuit characteristics are not a single number but a series of numbers corresponding to different normal modes of that element. The single circuit characteristics discussed in textbooks (say, the mutual capacitance between two conductors) correspond to that of the lowest mode. Such a description is valid only when the object can be considered as a single lumped element, in which the spatial charge (current) fluctuations are not important inside the object. In general, however, we need to know the characteristics for *all* normal modes. We illustrate below the calculations of such characteristics of a single metallic ring.

The studies of metallic ring-like systems[2–8] were stimulated by the discovery that a split ring resonator (SRR) processes a negative μ in some (microwave) frequency regimes[2] and thus can be employed to fabricate a LHM.[1] A naive approach to create a LHM at higher frequencies is to scale down the sizes of systems proven to work at lower frequencies.[9] However, the differences between various ring-like structures (single-ring, double-ring, one cut, two cuts, etc.)[1–9] are not yet completely clear. Since the experimental control of structures on a smaller scale is more limited, it is desirable to gain a complete theoretical understanding of the resonances in *arbitrary* metallic-ring-like systems.

In a pioneering paper,[2] Pendry *et al.* first pointed out that magnetic resonances exist in such SRR systems. However, Pendry *et al.* considered the ring as a single lumped element, described by single circuit characteristics, and approximated the mutual capacitance between two metallic rings by that for two infinitely large metallic sheets.[2] Later, Shamonin *et al.* modeled the system as an equivalent circuit consisting of an infinite number of lumped elements and set up a differential equation to describe the current-voltage relations on the rings.[4] This approach can handle the cases of nonuniform current (charge) distributions and therefore, has included an important part of local inductive/capacitive effects.[4] However, the latter were still not *completely* considered in that approach,[4] since in principle self (mutual) inductive/capacitive effects exist for any single (pair of) lumped element(s) inside the model. In addition, the approach still needs a set of empirical parameters that cannot be calculated rigorously,[4] such as the self-inductance of a single lumped element, the mutual capacitance between two lumped elements in two rings (denoted by C in Ref. 4), etc. Those values were determined under some approximations. For instance, the parameter C was again approximated by the mutual capacitance between two infinitely large metal plates.[4]

The SRR systems and their topological equivalents were also studied by numerical calculations.[6–8] Although such full-wave studies should in principle contain all relevant field information, sometimes it is not easy to analyze this information (usually presented as the transmission/reflection spectra), so as to extract the useful properties of a SRR from such information. For example, to obtain the effective ε and μ of a single SRR, one needs to perform complicated calculations on the transmission/reflection spectra obtained for a SRR array,[8] and even faces intrinsic difficulties in some cases (see footnote 12 in Ref. 10).

In this paper, within the quasistatic approximation (QSA),[11] we develop an alternative approach to study metallic ring systems. Compared to previous analytical approaches,[2–5] the present one considers the inductive/capacitive effects *completely* and calculates the involved circuit parameters *rigorously* rather than *empirically*. In addition, the approach provides us not only all the resonance frequencies but also the direct responses of the structure under an arbitrary probing field, which is complementary information to numerical approaches. This paper is organized as follows. After presenting all mathematic details of the theory in Sec. II, we applied it to study a single-ring SRR in Sec. III

as an illustration. We found that the even-numbered resonance modes of a single-ring SRR exhibit only electric responses, while the odd ones exhibit both electric and magnetic responses; the SRR possesses a bi-anisotropy at all odd-numbered resonances. We employed finite-difference-time-domain (FDTD) simulations[12] on realistic structures to successfully verify the predictions of the rigorous theory. In Sec. IV, we quantitatively compared our theory with previous empirical ones and discussed the applicability of the QSA, which is the only approximation adopted in this paper. After briefly introducing some other applications of the theory in Sec. V, we summarized our results in the last section.

II. BASIC THEORETICAL FORMALISMS

We consider a ring of radius R in the xy plane. In what follows, a common time-varying factor $\exp(i\omega t)$ is omitted for every quantity. Within the QSA,[11] the inductive field $\vec{E}_L(\vec{r})$ can be expressed in terms of the current $\vec{j}(\vec{r}')$ by Faraday's induction law,

$$\vec{E}_L(\vec{r}) = -\partial\vec{A}/\partial t = -i\omega\mu_0 \int \vec{j}(r')d\vec{r}'/(4\pi|\vec{r}-\vec{r}'|). \quad (1)$$

The capacitive field $\vec{E}_C(\vec{r})$ can be expressed in terms of the accumulated charges $\rho_e(\vec{r}')$ by Coulomb's law,

$$\vec{E}_C(\vec{r}) = -\nabla V(\vec{r}) = -\nabla \frac{1}{4\pi\varepsilon_0}\int \frac{\rho_e(\vec{r}')d\vec{r}'}{|\vec{r}-\vec{r}'|}$$

$$= \frac{1}{i\omega}\frac{1}{4\pi\varepsilon_0}\nabla \int \frac{[\nabla'\cdot\vec{j}(\vec{r}')]d\vec{r}'}{|\vec{r}-\vec{r}'|}, \quad (2)$$

where the current-charge conservation law $\nabla\cdot\vec{j}+\partial\rho_e/\partial t=0$ has been used.

We consider the thin-wire limit, $a \ll R$, where a is the radius of the metal wire forming the ring. In the frequency regime that we consider, the current flows on the conductor's outer surface within a layer of thickness of skin depth, so that $\vec{j}(\vec{r}')$ is basically a very complicated function of $\vec{r}'$. However, when the wire is very thin, we can simplify the realistic current distribution as a delta function localized in the middle of the wire, $\vec{j}(\vec{r}')=\vec{e}_\phi I(\phi)\sin\theta\delta(\cos\theta)\delta(r'-R)/R$ with $\vec{e}_\phi=-\sin\phi\vec{e}_x+\cos\phi\vec{e}_y$. This simplification will not generate any significant errors for calculating the fields outside the metal wire in the thin-wire limit. On the other hand, both $\vec{E}_L(\vec{r})$ and $\vec{E}_C(\vec{r})$ should still be calculated on the outer surface of the metal wire where the current *physically* flows. Again considering the fact $a \ll R$, we understand that $\vec{E}_L(\vec{r})$ and $\vec{E}_C(\vec{r})$ would not vary dramatically around the wire (as long as they are on the same position of the ring with a fixed ϕ), so that we can pick a particular (convenient) point on the wire surface to calculate these fields.

We expand the current as a Fourier series with respect to the azimuthal angle $I(\phi)=\Sigma_{m=-\infty}^{+\infty} I_m e^{im\phi}$ with $I_m=(1/2\pi)\int_0^{2\pi} I(\phi)e^{-im\phi}d\phi$. By expanding $1/|\vec{r}-\vec{r}'|$ in terms of spherical harmonics,[13]

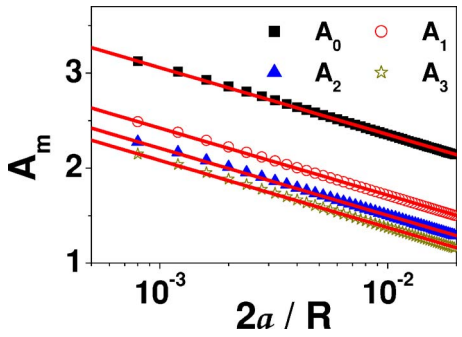

FIG. 1. (Color online) A_0, A_1, A_2, A_3 as functions of $2a/R$, calculated by directly evaluating infinite series (symbols). Lines are obtained by fitting to the formula $D_m+B_m\ln(2a/R)$. Here, $D_0=0.946$, $B_0=-0.3057$, $D_1=0.303$, $B_1=-0.3066$, $D_3=0.0894$, $B_3=-0.3069$, $D_4=-0.0389$, $B_4=-0.3070$.

$$\frac{1}{|\vec{r}-\vec{r}'|} = \sum_{l=0}\sum_{m=-l}^{l}\frac{4\pi}{2l+1}Y_{lm}(\theta,\phi)Y_{lm}^*(\theta',\phi')\frac{r_<^l}{r_>^{l+1}}, \quad (3)$$

with $r_<$ ($r_>$) being the smaller (larger) value of $|\vec{r}|$ and $|\vec{r}'|$, we can carry out the r' integration in Eq. (1) to obtain

$$E_L^m = -i\omega L_m I_m, \quad (4)$$

where

$$E_L^m = \frac{1}{2\pi}\int_0^{2\pi}\vec{E}_L\cdot\vec{e}_\phi \exp(-im\phi)d\phi \quad (5)$$

is the Fourier component of the inductive field, and

$$L_m = \mu_0(A_{m-1}+A_{m+1})/4 \quad (6)$$

is the inductance parameter

$$A_m = \sum_{l=|m|}^{\infty}\frac{(l-m)!}{(l+m)!}\alpha^l[P_l^m(0)]^2, \quad (7)$$

in which P_l^m is the associated Legendre function. Here we have $\alpha=(R-a)/R<1$, since we are calculating the field at a particular point $(r=R-a, \theta=\pi/2, \phi=\phi)$ on the wire surface. We can also take another position $(r=R+a, \theta=\pi/2, \phi=\phi)$ to do the calculations. In that case, we find that $\alpha=R/(R+a)$. It is worth noting that $(R-a)/R\approx R/(R+a)\approx 1-a/R$ in the thin-wire limit $a \ll R$, which justifies our previous arguments. We analyzed the series shown in Eq. (7) and found an asymptotic form $A_m\approx D_m-\ln(2a/R)/(\alpha^m\pi)$ in the limit of $a \ll R$. The numerical results for A_m as the functions of a/R are shown in Fig. 1, which unambiguously verifies the above asymptotical form (note that the values of B_m shown in the caption of Fig. 1 are quite close to the analytical value, $-1/\pi\approx-0.318$). We emphasize that this logarithmic divergence is a typical feature of many physical properties, including the self-inductance, of a thin-wire system.[14]

The capacitive term can be calculated similarly. After some straightforward calculations, we obtain

$$E_C^m = -I_m/(i\omega C_m), \quad (8)$$

where

$$E_C^m = \frac{1}{2\pi}\int_0^{2\pi} \vec{E}_C \cdot \vec{e}_\phi \exp(-im\phi)d\phi, \tag{9}$$

the Fourier component of the capacitive field, and

$$C_m = \frac{2\epsilon_0 R(R-a)}{m^2 A_m} \tag{10}$$

are the capacitance parameters. Note that $1/L_0C_1 \approx \omega_0^2$, where $\omega_0 = c_0/R$ is the angular frequency with wavelength as the ring perimeter, and $c_0 = 1/\sqrt{\varepsilon_0\mu_0}$ is the speed of light. ω_0 is the frequency unit of the present problem.

According to Ohm's law, the induced current $\vec{j}(\vec{r})$ is driven by the sum of the external field $\vec{E}_{ext}(\vec{r})$, the inductive and the capacitive fields. In Fourier component form we get

$$\sum_{m'} \tilde{\rho}(m-m')I_{m'} = E_{ext}^m + E_L^m + E_C^m = E_{ext}^m - i\omega L_m I_m - I_m/i\omega C_m, \tag{11}$$

where $\tilde{\rho}(m-m')$ is the Fourier component of $\tilde{\rho}(\phi) = \rho(\phi)/S$, the resistivity $\rho(\phi)$ normalized by the area S through which the current flows. The displacement current is omitted in writing Eq. (11), which is consistent with the QSA. We will discuss the applicability of this approximation in Sec. IV.

Equation (11) can be written as

$$\sum_{m'} H_{mm'}I_{m'} = E_{ext}^m, \tag{12}$$

where

$$H_{mm'} = \tilde{\rho}(m-m') + i\omega L_m(1-\Omega_m^2/\omega^2)\delta_{mm'}, \tag{13}$$

with

$$\Omega_m = 1/\sqrt{L_m C_m} = |m|\omega_0\sqrt{2A_m/\alpha(A_{m-1}+A_{m+1})}. \tag{14}$$

We note that $\Omega_m \to |m|\omega_0$ in the limit of $a/R \to 0$. We diagonalize the H matrix through

$$\tilde{H} = P^{-1}HP, \quad \tilde{I} = P^{-1}I, \quad \tilde{E}_{ext} = P^{-1}E_{ext}, \tag{15}$$

and get

$$\tilde{I}_m = \frac{\tilde{E}_{ext}^m}{\lambda_m(\omega)}, \tag{16}$$

where λ_m is the mth eigenvalue of the H matrix. We numerically determine the resonance frequencies by the condition that the magnitude of the lowest eigenvalue of the matrix H exhibits a minimum.

III. APPLICATIONS TO A SRR

We consider a single-ring SRR to illustrate our ideas. We set the resistivity of the metal as 0, and that of the air gap as $\tilde{\rho}_0$,

$$\tilde{\rho}(\phi) = \begin{cases} \tilde{\rho}_0, & \phi \in [-\Delta/2, \Delta/2], \\ 0, & \text{elsewhere}. \end{cases} \tag{17}$$

We take a very large value of $\tilde{\rho}_0$ in our numerical calculations and consider the limit $\tilde{\rho}_0 \to \infty$ later. The magnitude of the lowest eigenvalue is shown as a function of frequency in Fig. 2 for a typical SRR with $\Delta = \pi/40$ and $\alpha = 0.99$. The general agreements among different sets of calculations show that the adopted approximations, namely, taking finite values of angular momentum cutoff $M_{\max}$ and the gap resistivity parameter $\tilde{\rho}_0$, do not introduce any significant errors. The series of resonances in Fig. 2 can be categorized into two classes.[15] The even-numbered resonances ω_{2i} coincide well with the intrinsic resonances defined in Eq. (15), Ω_i, indicating that these resonances might be solely determined by the ring geometry. The odd-numbered ones, however, must be introduced by the air gap through the term $\tilde{\rho}(m-m')$. The eigenvectors [contained in the matrix P defined in Eq. (15)] are shown in Fig. 3 for the lowest four resonances. The odd-numbered (even-numbered) resonance modes possess symmetrical (antisymmetrical) eigenvectors with respect

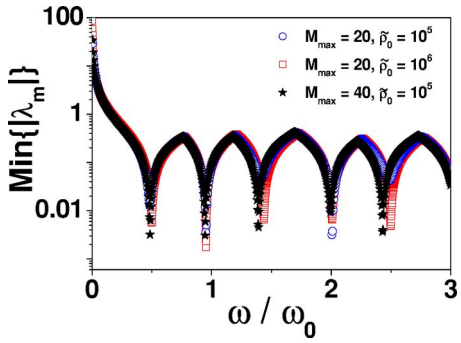

FIG. 2. (Color online) Min[$|\lambda_m|$] as functions of ω/ω_0, calculated with different values of $M_{\max}$ and $\tilde{\rho}_0$ (in units of $\mu_0\omega_0$).

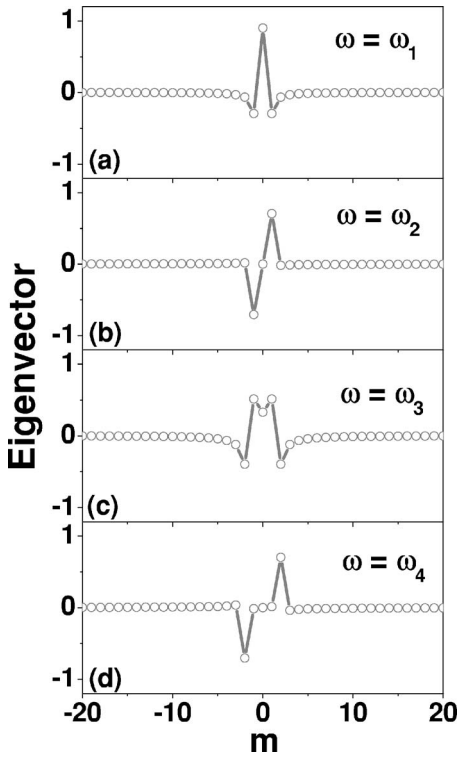

FIG. 3. The eigenvector distributions for the lowest eigenmode at the lowest four resonance frequencies.

to index m. A simple three-mode approximation for the lowest resonance gives $\omega=[L_1/(2L_0+L_1)]^{1/2}\Omega_1\approx\Omega_1/\sqrt{3}$, in reasonable agreement with the numerical results.

With the knowledge of the eigenvectors, we can further evaluate the electric and magnetic responses of the system. According to Eqs. (15) and (16), we find the SRR to possess the following nonzero components of dipole moments:

$$p_x=\sum_j \frac{1}{\lambda_j(\omega)}\frac{\pi R}{\omega}[P_{-1j}-P_{1j}]\cdot\tilde{E}^j_{ext},$$

$$p_y=\sum_j \frac{1}{\lambda_j(\omega)}\frac{\pi R}{i\omega}[P_{-1j}+P_{1j}]\cdot\tilde{E}^j_{ext},$$

$$m_z=\sum_j \frac{\pi R^2}{\lambda_j(\omega)}P_{0j}\cdot\tilde{E}^j_{ext}, \tag{18}$$

where

$$\tilde{E}^j_{ext}=\sum_l (P^{-1})_{jl}E^l_{ext}$$

$$=\frac{1}{2\pi}\int\sum_l (P^{-1})_{jl}\vec{E}_{ext}(\vec{r})\cdot\vec{e}_\phi\exp(-il\phi)d\phi \tag{19}$$

represents the external field component projected on the jth eigenmode. We consider the following four types of external probing fields, which are plane waves with polarization (**E** field direction) and wave propagating direction given by (a) $\vec{E}\|\hat{y},\vec{k}\|\hat{z}$, (b) $\vec{E}\|\hat{y},\vec{k}\|\hat{x}$, (c) $\vec{E}\|\hat{x},\vec{k}\|\hat{z}$, and (d) $\vec{E}\|\hat{x},\vec{k}\|\hat{y}$ ($\vec{k}$ is the wave vector). The moment amplitudes under these probing fields are respectively shown in Fig. 4 as functions of the reduced frequency. The odd-numbered resonance modes possess both magnetic (m_z) and electric (p_y) responses, while the even-numbered ones possess only electric (p_x) responses. The appearance of p_y is always accompanied by the appearance of m_z. This bi-anisotropy property of the SRR has been proposed and studied previously but only for the lowest mode.[5,7] Here, we rigorously demonstrate that the bi-anisotropy is the system's intrinsic property at all odd-numbered resonances. Symmetry restricts a probing field to excite only a particular set of resonance modes of the SRR. Taking configuration (a) as an example, since the probing field projected on the ring, $E_{ext}(\phi)=\vec{E}_{ext}\cdot\hat{e}_\phi=E_0\cos\phi$, exhibits an even symmetry with respect to ϕ, only the odd-numbered modes possessing even-symmetry current distributions (see Fig. 3) can be excited. Similar arguments hold for other configurations.

We have performed FDTD simulations on realistic structures to verify the above predictions. To model a single-ring SRR with $R=4$ mm, $a=0.1$ mm, and $\Delta=\pi/40$, we first construct a 0.2 mm thick metallic disk of radius 4.1 mm, then cut it by a 0.2 mm thick air disk of radius 3.9 mm, and finally cut an air gap of the required width on the resulting structure. It is difficult to employ FDTD simulations to directly compute the dipole moments of a single SRR induced by an external plane wave. Instead, we study the transmission spectrum of an array of such SRR's, and identify the resonances by the dips of the transmission spectrum. For the

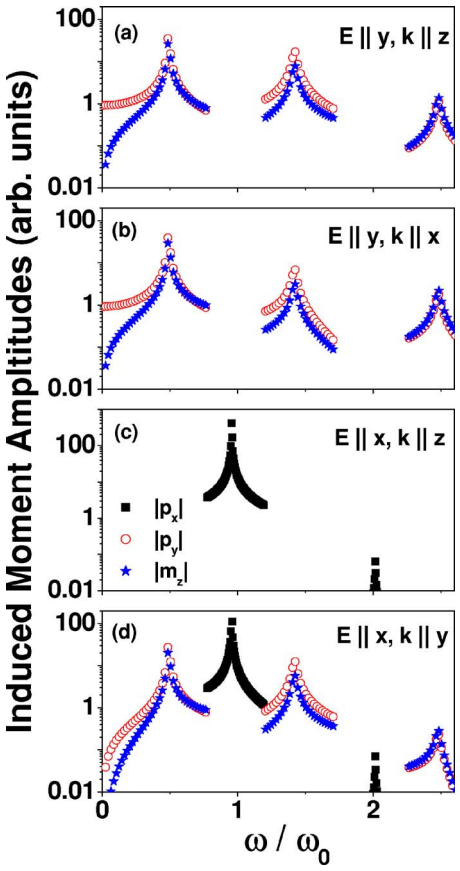

FIG. 4. (Color online) Amplitudes of the induced moments, $|p_x|$, $|p_y|$, $|m_z|$, of the SRR as functions of ω/ω_0 for different probing fields as shown in the figure.

two configurations studied in Figs. 4(a) and 4(c), we construct SRR arrays to periodically tile the xy plane, with lattice constants 16 mm along both x and y directions. For the other two configurations, we construct SRR arrays to periodically tile the xy or yz plane, respectively, with a lattice constant =12 mm along x or y direction and 16 mm along z direction. The transmission spectra[16] under the four plane wave inputs are shown, respectively, in Figs. 5(a)–5(d). When we compare Fig. 5 with the results shown in Fig. 4, we find that they agree with each other quite well.[17] We clearly identify the dips at $\omega\approx0.42\omega_0$ shown in Figs. 5(a), 5(b), and 5(d) as the lowest eigen resonance mode (ω_1), the dips at $\omega\approx1.19\omega_0$ shown in Figs. 5(c) and 5(d) as the second resonance mode (ω_2), and the dips at $\omega\approx1.46\omega_0$ as the third one (ω_3).

IV. FURTHER DISCUSSIONS ON THE THEORY

In this section we will compare our theory with previous analytical ones and discuss the applicability of the QSA, which is the only approximation adopted in the present theory.

As it is tedious to reproduce the results by Shamonin *et al.*,[4] we will compare our theory with the pioneering work by Pendry *et al.*[2] In Ref. 2, Pendry *et al.* considered a double split-ring system and found that the system possesses a mag-

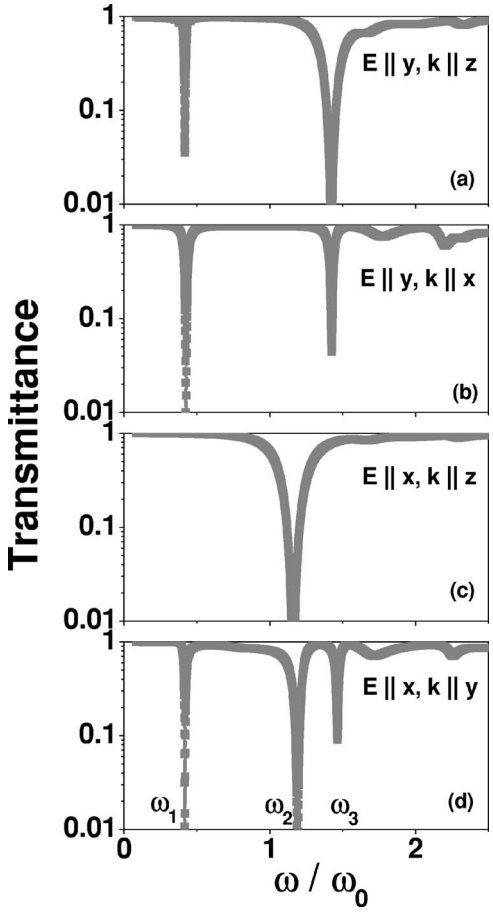

FIG. 5. FDTD calculated transmission spectra of the SRR arrays (explained in the text) as functions of ω/ω_0 for plane wave inputs specified in the figure.

netic resonance with frequency determined by

$$\omega_0 = \sqrt{\frac{3dc_0^2}{\pi^2 R^3}}, \tag{20}$$

where d is the space between two split rings. In order to compare with the present results, we examine the properties of the single-ring SRR limit of Pendry's approach. Naively, we expect that the double-ring SRR becomes two independent single-ring SRR's as $d \to \infty$, where the inner ring remains unchanged and the outer ring becomes too large to be relevant. Therefore, inserting $d \to \infty$ into Eq. (20) should generate the results for a single-ring (i.e., the inner ring) SRR with radius given by R. However, when we put $d \to \infty$ into Eq. (20), we find that the resonance frequency approaches infinity, in apparent disagreement with the numerical results shown in Fig. 5. That there is only one resonance in such a system is also inconsistent with the numerical results shown in Fig. 5. Such discrepancies are caused by the fact that Pendry *et al.* only considered the mutual capacitance between two rings but neglected the self-capacitance effect of a single ring caused by the gap and neglected the capacitance/inductance effects for all higher order modes. In contrast, our theory has considered the capacitive/inductive effects completely and thus can be compared with the full-wave simulation results successfully, without taking any empirical parameters.

Our theory is developed under the QSA. Within such an approximation,[11] we neglected the displacement current in writing Eq. (11) and the radiation effects in writing Eqs. (1) and (2). Omission of the displacement current in Eq. (11) is well justified for the present problems, since the realistic current inside a good metal is much larger than the displacement current in the frequency regime considered here.[11] We now consider the radiation corrections to Eqs. (1) and (2). If the radiation effects are fully included, Eq. (1) should read

$$\vec{E}_L^F(\vec{r}) = -i\omega\mu_0 \int \frac{\vec{j}(r')\exp[i\omega|\vec{r}-\vec{r}'|/c_0]}{4\pi|\vec{r}-\vec{r}'|} d\vec{r}'. \tag{21}$$

Compared with Eq. (1), one may argue that the QSA is applicable only when the condition

$$\max[\omega|\vec{r}-\vec{r}'|/c_0] = \omega 2R/c_0 = 2\omega/\omega_0 \ll 1 \tag{22}$$

is fulfilled. However, the comparison between the theory and numerical simulations (with radiation effects fully included) suggested that the applicable regime of the QSA is much wider than that indicated by the condition (22), as shown in last section. We believe that condition (22) is too strict for such problems, particularly in the thin-wire limit. Since we are calculating the electric fields on the wire surface, the dominant contributions to the integration (21) come from those points $\vec{r}'$ that are very close to $\vec{r}$. For such points $\omega|\vec{r}-\vec{r}'|/c_0 \ll 1$ and the radiation corrections are very small. Therefore, the QSA has considered correctly the most dominant part of the contribution and neglected those radiation corrections which are less important. Let us check the radiation correction to the inductive field,

$$\Delta\vec{E}_L(\vec{r}) = \vec{E}_L^F(\vec{r}) - \vec{E}_L(\vec{r}) = -i\omega\mu_0 \int \frac{\vec{j}(r')}{4\pi|\vec{r}-\vec{r}'|} \times\{\exp[i\omega|\vec{r}-\vec{r}'|/c_0]-1\}d\vec{r}'. \tag{23}$$

Since $\{\exp[i\omega|\vec{r}-\vec{r}'|/c_0]-1\}/|\vec{r}-\vec{r}'|_{\vec{r}\to\vec{r}'} \to i(\omega/c_0)$, the integration (23) becomes convergent in the $a \to 0$ limit. Considering the logarithmic divergence of the function A_m and hence E_L, we find that

$$\frac{|\Delta\vec{E}_L(\vec{r})|}{|\vec{E}_L(\vec{r})|} \to \frac{\text{const.}}{\ln(2a/R)} \to 0, \quad \text{as } \frac{a}{R} \to 0. \tag{24}$$

Equation (24) indicates that the radiation corrections are indeed negligible in the limit of $a \to 0$ for such problems, and as the result, our theory becomes exact in the limit of $a \to 0$. For a finite value of a, there exists a finite frequency regime for the QSA to be applicable. Nevertheless, such a regime should still be much wider than that indicated by condition (22), which is too strict for the present problem.

Li *et al.*[18] provided a general representation to rigorously calculate the radiation fields of a current-carrying metallic ring, which is an active element with current distribution predetermined. Our theory calculates the responses of a metallic ring system under an arbitrary external field in which the metallic ring is a passive element whose current distribu-

tion is unknown and is what we are interested in. To derive the system's responses from Li *et al.*'s theory,[18] one needs to calculate the total fields (both the radiation fields from the current loop itself and any other external fields) on the wire surface and then determine the current distribution through Ohm's law self-consistently. This is precisely the contribution of the present work. Certainly, it is worthwhile to employ Li *et al.*'s representation[18] to incorporate the radiation corrections into our theory, which will be an interesting issue for future works.

V. OTHER POSSIBLE APPLICATIONS

The present "rigorous" theory is applicable to many other situations. Below we sketch some examples. For two concentric rings of radii R' and R $(R'>R)$, we find that the mutual inductance $\tilde{L}_m$ is the same as L_m except that A_m should be replaced by $\tilde{A}_m=\Sigma_{l=|m|}^{\infty}[(l-m)!/(l+m)!]\tilde{\alpha}^l[P_l^m(0)]^2$ with $\tilde{\alpha}=R/R'$, and the mutual capacitance is now $\tilde{C}_m=2\epsilon_0 RR'/m^2\tilde{A}_m$. The interactions between rings make the eigenmode structures even intriguing. For example, consider a standard double-ring SRR with two cuts on opposite sides of the two rings. If we assume the same self-inductances and capacitances of the two rings (valid for $R\approx R'$), in a three-mode approximation we find that the resonance frequencies for the lowest two modes are given by $\omega_{\pm}=\sqrt{(L_1\Omega_1^2\pm\tilde{L}_1\tilde{\Omega}_1^2)/(L_1\pm\tilde{L}_1+2L_0\mp 2\tilde{L}_0)}$, and the current distributions in the two rings are given by $j\approx j_0[-1+\cos\phi]$ and $j'\approx\pm j_0[1+\cos\phi]$. While both modes exhibit bi-anisotropy, for the higher (lower) frequency optical (acoustic) mode, the magnetic (electric) m_z (p_y) response is significantly reduced, leaving the net response much more electric (magnetic) in character.

To apply the present theory to study the SRR arrays, we need to consider the mutual-inductance and capacitance between two metallic rings located at arbitrary positions. We find that analytical formulations can be obtained for some special configurations with high symmetries. For example, consider two identical rings (with radius R) placed on different xy planes, whose centers are separated by a distance d on the z axis. For this system, the mutual inductance $L'_m(d)$ is found to be the same as Eq. (6), with A_m replaced by $A'_m(d)=\Sigma_{l=|m|}^{\infty}[(l-m)!/(l+m)!](\alpha')^{l+1}[P_l^m(0)]^2$ in which $\alpha'=R/\sqrt{R^2+d^2}$, and the mutual capacitance is found as $C'_m(d)=2\varepsilon_0 R\sqrt{R^2+d^2}/m^2A'_m$. It is clear that the inter-ring interactions are decreasing functions of the separation d, consistent with our naïve expectations. With these parameters, we can in principle investigate the eigenmode properties of a special SRR array, in which the centers of rings are on the same z axis. However, for a general type of periodic SRR array, analytical formulations are difficult to obtain and we have to seek help from numerical simulations.[6–8]

We can also study the effect of absorption in the SRR systems. The dissipation rate in such a system is found as

$$\frac{dQ}{dt}=\frac{1}{2}\int \mathrm{Re}\{[\vec{E}_{ext}(\vec{r},t)]^*\vec{j}(\vec{r},t)\}d\vec{r}=\pi R\sum_m \mathrm{Re}[(E_{ext}^m)^*I_m]. \tag{25}$$

In the limit of $\tilde{\rho}_0\to\infty$ that we consider, the H matrix (13) is essentially a Hermitian matrix, so we can prove that

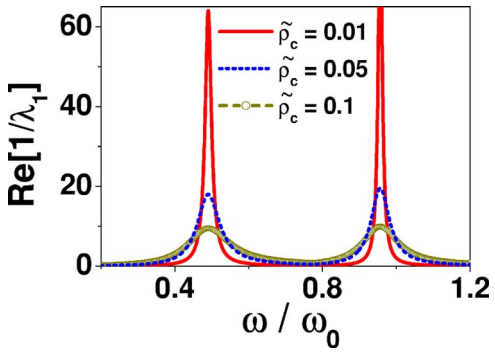

FIG. 6. (Color online) $\mathrm{Re}[1/\lambda_1]$ [in units of $(\mu_0\omega_0)^{-1}$] as functions of ω/ω_0 calculated with different values of $\tilde{\rho}_c$ (in units of $\mu_0\omega_0$) specified in the legend. Here we set $\tilde{\rho}_0=10^5\mu_0\omega_0$.

$$\frac{dQ}{dt}=\pi R\sum_m |\tilde{E}_{ext}^m|^2\mathrm{Re}\left[\frac{1}{\lambda_m}\right]. \tag{26}$$

Therefore, the real parts of eigenvalues are intimately related to the absorption in such systems. Take a single-ring SRR as an example. Suppose the conductor forming the ring has a finite resistivity $\tilde{\rho}_c$, the resistivity function then becomes

$$\tilde{\rho}(m-m')=\begin{cases}\dfrac{\sin[(m-m')\Delta/2]}{\pi(m-m')}(\tilde{\rho}_0-\tilde{\rho}_c), & m\neq m',\\ \tilde{\rho}_c+\dfrac{\Delta}{2\pi}(\tilde{\rho}_0-\tilde{\rho}_c), & m=m'.\end{cases} \tag{27}$$

Inserting Eq. (27) to Hamiltonian (13) and solving the matrix, we obtain a series of eigenvalues $\{\lambda_m\}$ as the functions of frequency. We label the eigenmode with the lowest eigenvalue by index 1 and depict the values of $\mathrm{Re}[1/\lambda_1(\omega)]$ in Fig. 6 as the functions of frequency, calculated with different values of $\tilde{\rho}_c$. Since $|\tilde{E}_{ext}^m|^2$ are positive-definite numbers and $\mathrm{Re}[1/\lambda_1(\omega)]$ is the largest one among $\mathrm{Re}[1/\lambda_m(\omega)]$, we understand that the spectra shown in Fig. 6 are closely related to the true absorption spectra. When $\tilde{\rho}_c$ is small, we find that the absorption is significant only at the vicinities of resonance. As $\tilde{\rho}_c$ increases, the absorption spectrum is obviously smeared out. All these are very typical features of resonance behaviors. We note that the exact value of the dissipation rate depends on the concrete form of the external probing field.

Other elements such as disks and spheres can also be studied from this perspective. The scattering from spheres obtained by matching the tangential components of E and H fields at the boundary is well known, but only for the case with uniform conductivity. The current approach provides a way to study the situations with nonuniform conductivity.

VI. CONCLUSIONS

We have established an analytical theory within the quasistatic approximation to study the EM properties of metallic ring-like systems. The theory is "rigorous" in the sense that we have incorporated the capacitive and inductive effects completely and have calculated the involved parameters rig-

orously. The application to a single-ring SRR uncovers rich properties of its eigenmodes, which are successfully verified by FDTD simulations on realistic structures. We have discussed the applicability of the quasistatic approximation adopted in our theory and found that the approximation becomes exact in the thin-wire limit. Other possible applications are also briefly discussed.

ACKNOWLEDGMENTS

This work was supported by the National Basic Research Program of China (No. 2004CB719800), the NSFC (No. 1050400310321003), Shanghai Science and Technology Committee (Nos. 05PJ14021 and 05JC14061), Fok Ying Tung Education Foundation, and PCSIRT. S.T.C. was partly supported by the NSF.

*Author to whom correspondence should be addressed. Electronic address: phzhou@fudan.edu.cn

[1] V. C. Veselago, Sov. Phys. Usp. **10**, 509 (1968); D. R. Smith, W. J. Padilla, D. C. Vier, S. C. Nemat-Nasser, and S. Schultz, Phys. Rev. Lett. **84**, 4184 (2000); R. A. Shelby, D. R. Smith, and S. Schultz, Science **292**, 77 (2001).

[2] J. B. Pendry, A. J. Holden, D. J. Robbins, and W. J. Stewart, IEEE Trans. Microwave Theory Tech. **47**, 2075 (1999).

[3] J. Zhou, Th. Koschny, M. Kafesaki, E. N. Economou, J. B. Pendry, and C. M. Soukoulis, Phys. Rev. Lett. **95**, 223902 (2005).

[4] M. Shamonin, E. Shamonina, V. Kalinin, and L. Solymar, J. Appl. Phys. **95**, 3778 (2004).

[5] R. Marques, F. Medina, and R. Raffi-El-Idrissi, Phys. Rev. B **65**, 144440 (2002); R. Marques, F. Mesa, J. Martel, and F. Medina, IEEE Trans. Antennas Propag. **51**, 2572 (2003).

[6] D. R. Smith, S. Schultz, P. Markos, and C. M. Soukoulis, Phys. Rev. B **65**, 195104 (2002).

[7] N. Katsarakis, T. Koschny, M. Kafesaki, E. N. Economou, and C. M. Soukoulis, Appl. Phys. Lett. **84**, 2943 (2004).

[8] P. Markos and C. M. Soukoulis, Phys. Rev. E **65**, 036622 (2002); Bogdan-Ioan Popa and S. A. Cummer, Phys. Rev. B **72**, 165102 (2005).

[9] T. J. Yen, W. J. Padilla, N. Fang, D. C. Vier, D. R. Smith, J. B. Pendry, D. N. Basov, and X. Zhang, Science **303**, 1494 (2004); S. Linden, C. Enkrich, M. Wegener, J. F. Zhou, T. Koschny, and C. M. Soukoulis, Science **306**, 1351 (2004).

[10] J. Li, L. Zhou, C. T. Chan, and P. Sheng, Phys. Rev. Lett. **90**, 083901 (2003).

[11] J. D. Jackson, *Classical Electrodynamics*, 3rd ed. (Wiley, New York, 1999), Sec. 5.18.

[12] K. S. Yee, IEEE Trans. Antennas Propag. **14**, 302 (1966).

[13] J. D. Jackson, *Classical Electrodynamics*, 3rd ed. (Wiley, New York, 1999), Sec. 3.5.

[14] J. D. Jackson, *Classical Electrodynamics*, 3rd ed. (Wiley, New York, 1999), Sec. 5.17.

[15] $|\lambda_m|$ is not exactly 0 at the resonance frequencies, due to the finite resistivity $\tilde{\rho}_0$ and cutoff parameter $M_{\max}$ adopted here. We expect that $|\lambda_m|$ reaches zero exactly at the resonance frequencies in the limit of $\tilde{\rho}_0, M_{\max} \to \infty$.

[16] Simulations were performed using the package CONCERTO 4.0, developed by Vector Fields, Limited, England, 2005. We have applied the perfect-metal boundary conditions for the air/metal interfaces. A basic cell sized 0.15 mm $\times$ 0.15 mm $\times$ 0.25 mm is employed to discretize the structure, and we have adopted finer meshes wherever necessary.

[17] We cannot unambiguously identify the modes with order higher than three since their strengths are too weak. The resonance frequencies do not perfectly match the theoretical values suggested in Fig. 2, which is suspected to be caused by the interactions between adjacent SRR's in the periodic array.

[18] L. W. Li, M. S. Leong, P. S. Kooi, and T. S. Yeo, IEEE Trans. Antennas Propag. **45**, 1741 (1997).